Carcinogenesis vol.34 no.9 pp.2119–2128, 2013
doi:10.1093/carcin/bgt143
Advance Access publication April 30, 2013

RIP1 potentiates BPDE-induced transformation in human bronchial epithelial cells through catalase-mediated suppression of excessive reactive oxygen species

Qiong Wang[1,2], Wenshu Chen[2], Xiuling Xu[2], Bilan Li[2], Weiyang He[2], Mabel T.Padilla[2], Jun-Ho Jang[2,3], Toru Nyunoya[2,3], Shantu Amin[4], Xia Wang[1] and Yong Lin[2,*]

[1]Laboratory of Molecular and Translational Medicine, West China Second University Hospital, Sichuan University, Chengdu 610041, China, [2]Molecular Biology and Lung Cancer Program, Lovelace Respiratory Research Institute, 2425 Ridgecrest Drive South East, Albuquerque, NM 87108, USA, [3]Division of Pulmonary and Critical Care Medicine, University of New Mexico and New Mexico Veterans Affairs Health Care System, Albuquerque, NM 87108, USA and [4]Department of Pharmacology, Penn State Hershey College of Medicine, Hershey, PA 17033, USA

*To whom correspondence should be addressed. Tel: +1 505 348 9645;
Fax: +1 505 348 4990;
Email: ylin@lrri.org
Correspondence may also be addressed to Xia Wang. Tel: +86 28 85503771;
Fax: +86 28 85503604;
Email: xiawang@scu.edu.cn

Cell survival signaling is important for the malignant phenotypes of cancer cells. Although the role of receptor-interacting protein 1 (RIP1) in cell survival signaling is well documented, whether RIP1 is directly involved in cancer development has never been studied. In this report, we found that RIP1 expression is substantially increased in human non-small cell lung cancer and mouse lung tumor tissues. RIP1 expression was remarkably increased in cigarette smoke-exposed mouse lung. In human bronchial epithelial cells (HBECs), RIP1 was significantly induced by cigarette smoke extract or benzo[a]pyrene diol epoxide (BPDE), the active form of the tobacco-specific carcinogen benzo(a)pyrene. In RIP1 knockdown HBECs, BPDE-induced cytotoxicity was significantly increased, which was associated with induction of cellular reactive oxygen species (ROS) and activation of mitogen-activated protein kinases (MAPKs), including c-jun N-terminal kinase (JNK), extracellular signal-regulated kinase (ERK) and p38. Scavenging ROS suppressed BPDE-induced MAPK activation and inhibiting ROS or MAPKs substantially blocked BPDE-induced cytotoxicity, suggesting ROS-mediated MAPK activation is involved in BPDE-induced cell death. The ROS-reducing enzyme catalase is destabilized in an ERK- and JNK-dependent manner in RIP1 knockdown HBECs and application of catalase effectively blocked BPDE-induced ROS accumulation and cytotoxicity. Importantly, BPDE-induced transformation of HBECs was significantly reduced when RIP1 expression was suppressed. Altogether, these results strongly suggest an oncogenic role for RIP1, which promotes malignant transformation through protecting DNA-damaged cells against carcinogen-induced cytotoxicity associated with excessive ROS production.

Introduction

Cancer arises from cells that have acquired genetic mutations and epigenetic alterations caused by carcinogens. Only a small fraction of cells with carcinogen-induced DNA damage are eventually transformed to be malignant because genotoxic stresses activate DNA repair pathways to retain genomic integrity and apoptosis pathways to eliminate genetically damaged cells. Thus, it is believed that carcinogenesis is likely dependent on the balance between cell survival and apoptosis signals, both of which are activated by carcinogens (1). The pathways controlling survival and death, including mitogen-activated protein kinases (MAPKs), Akt and nuclear factor-kappaB (NF-κB), are mediated by receptor-interacting protein 1 (RIP1) (2–4). However, whether RIP1 plays a role in lung carcinogenesis has never been investigated.

Initially identified as a Fas-interacting protein and an adaptor protein in the tumor necrosis factor (TNF) receptor 1 signaling complex for NF-κB activation, RIP1 is believed to be a mediator for cell survival. RIP1 mediates cell survival signaling pathways activated by a variety of extracellular and intracellular stimulations and stresses as follows: NF-κB activation mediated by death receptors (5–7), Toll-like receptors and genotoxic stress (8,9), and Akt activation mediated by Toll-like receptors (10,11). Because increased cell survival capacity is a hallmark of cancer cells, cell survival pathways are believed to be targets for cancer chemotherapy (1). Indeed, Hsp90 inhibitor-mediated destruction of RIP1 protein potently blocked NF-κB and potentiated TNF- or tumor necrosis factor-related apoptosis-inducing ligand-induced cancer cell death (12–14). However, recent studies indicate a pro-death role for RIP1, which involves both apoptosis and necrosis induced by TNF and genotoxic stresses (15–18). In fact, RIP1 also mediates activation of MAPKs, which can be involved in either cell survival or death (3,19–21). Therefore, RIP1 is at a unique position to relay signals activated by diverse stimuli to different pathways for either cell survival or death. How RIP1-mediated contradictory cellular signaling is regulated is not well understood, but modifications to RIP1 such as phosphorylation and ubiquitination and cleavage of RIP1 may control interactions of RIP1 with its partners and subsequent functions (22,23). The cellular outcome mediated by RIP1 might depend on cell context and stimulation types (2,4,9,24).

RIP1 overexpression was found in glioblastoma, which was associated with worse prognosis (25). RIP1 was also able to activate NF-κB and Akt, and inhibit p53 in glioblastoma cells (25,26). However, due to the complex functions of RIP1 in cell signaling, whether RIP1 is involved and what the role of RIP1 is in carcinogenesis are still elusive. In this report, we found that RIP1 expression is increased in human lung cancer tissues and cell lines. Cigarette smoke extract (CSE) and the benzo[a]pyrene diol epoxide (BPDE), the active form of the tobacco-specific carcinogen benzo(a)pyrene, strongly induced RIP1 expression in human bronchial epithelial cells. When RIP1 was knocked down, BPDE-induced and ROS-mediated cytotoxicity was significantly increased and cell transformation was significantly reduced. These results strongly suggest a tumor-promoting role for RIP1, which promotes malignant transformation through protecting DNA-damaged cells against carcinogen-induced cytotoxicity that is associated with excessive ROS production.

Abbreviations: BHA, butylated hydroxyanisole; BPDE, benzo[a]pyrene diol epoxide; CS, cigarette smoking; CSE, cigarette smoke extract; ERK, extracellular signal-regulated kinase; HBEC, human bronchial epithelial cell; JNK, c-jun N-terminal kinase; LDH, lactate dehydrogenase; MAPK, mitogen-activated protein kinase; NAC, *N*-acetyl-L-cysteine; NF-κB, nuclear factor-kappaB; RIP1, receptor-interacting protein 1; ROS, reactive oxygen species; shRNA, short hairpin RNA; TNF, tumor necrosis factor.

Materials and methods

Reagents

BPDE was obtained from laboratory of S.A. (27,28). CSE was prepared by sequentially extracting materials from filters, which were collected from the AMESA Type 1300 smoking machine generating mainstream cigarette smoke, with dimethyl sulfoxide (for dissolving water-insoluble components) and keratinocyte serum-free medium (for dissolving water-soluble components). The water-soluble and water-insoluble fractions were stored at −80°C and proportionally mixed to make total CSE before use. Total particulate material was determined by weighing the filter before and after extraction. Antibodies against RIP1, Mn-SOD and JNK were from

BD Biosciences (San Diego, CA). Anti-phospho-JNK and ERK were from Invitrogen (Camarillo, CA). Anti-phospho-p38, p38, ERK and catalase were purchased from Cell Signaling (Beverly, MA). The inhibitors, SP600125 for JNK, U0126 for ERK and SB203580 for p38, were from Calbiochem (La Jolla, CA). Butylated hydroxyanisole (BHA) and *N*-acetyl-L-cysteine (NAC) were from Sigma (St Louis, MO). 5-(and-6)-Chloromethyl-2′,7′-dichlorodihydro fluorescein diacetate, acetyl ester and Amplex red catalase assay kit (A22180) were purchased from Molecular Probes (Eugene, OR). Catalase from bovine liver was from Sigma–Aldrich.

Cell culture

Immortalized human bronchial epithelial cells, HBEC-2, HBEC-13 and BEAS-2B, were generously provided by Drs Shay and Minna, Southwestern Medical Center, Dallas, TX (29), and cultured in keratinocyte serum-free medium supplemented with 5 μg/l of human recombinant epidermal growth factor and 50 mg/l of bovine pituitary extract (Invitrogen) in plates coated with FNC coating mix (Athena ES). All cells were grown under standard incubator condition at 37°C and with 5% CO_2.

Tissue array and immunohistochemistry

Human lung cancer tissue microarray slides containing human lung tumors and normal lung tissues were purchased from Imgenex. Immunohistochemistry was carried out using the VECTASTAIN® ABC Kit with peroxidase labeling and DAB (3,3′-diaminobenzidine) Peroxidase Substrate Kit from Vector (Burlingame, CA). Briefly, the slides were deparaffinized in xylene and rehydrated in diluted ethanol. Antigen retrieval was done by boiling the slide in 0.1% citrate buffer for 15 min, and the slide was then treated with 3% H_2O_2 for 20 min followed by blocking with 5% normal rabbit serum in phosphate-buffered saline for 2 h at room temperature. Subsequently, the slide was incubated with primary antibody (rabbit anti-RIP1, Geneway, 1:800) overnight at 4°C. The ABC kit was then applied, and the slide was developed with 3,3′-diaminobenzidine according to instructions from the manufacturer. The staining of RIP1 in tumor was compared with the corresponding adjacent or a group of normal tissues on the same slide. The expression of RIP1 in tumor tissue was regarded as 'normal' if the staining was comparable with normal tissues, or 'increased' when the staining was stronger in tumor than that in normal tissue.

Western blot

Cells were treated as indicated in each figure legend, and cell lysates were prepared by lysing cells in M2 buffer [20 mM Tris–HCl (pH 7.6), 0.5% NP40, 250 mM NaCl, 3 mM ethylenediaminetetraacetic acid, 3 mM ethyleneglycol-bis(aminoethylether)-tetraacetic acid, 2 mM dithiothreitol, 0.5 mM phenylmethylsulfonyl fluoride, 20 mM β-glycerophosphate, 1 mM sodium vanadate and 1 μg/ml leupeptin]. Equal amounts of protein from each cell lysate were resolved by 12% or 15% sodium dodecyl sulfate–polyacrylamide gel electrophoresis and transferred to a polyvinylidene fluoride membrane, then analyzed by western blot using various antibodies. The proteins were visualized by enhanced chemiluminescence (Millipore), according manufacturer's instructions.

Knockdown of RIP1 expression by RNAi

The RIP1 short hairpin RNA (shRNA)-expressing plasmid was constructed by inserting a synthetic oligonucleotide encoding a hairpin sequence with a 19-nucleotide stem that is homologous to the target sequence of human RIP1, AGGTCATGTTCTTTCAGCTTA, and a 9-base loop sequence into pSilencer 4.1-CMV hygro at the BamHI site (Oligoengine). HBEC-2 and HBEC-13 cells were transfected with pSilencer 4.1-CMV-hygro-RIP1shRNA using FuGENE HD transfection reagent (Promega), following the manufacturer's instruction. Cell clones with stable RIP1 knockdown were selected with hygromycin (25 μg/ml) and confirmed by western blot. Cells stably transfected with pSilencer 4.1-CMV-hygro were selected with hygromycin and pooled and used as negative control cells.

Cytotoxicity assay

Cells were seeded in 48-well plate 1 day before treatment and then treated as indicated in each figure legend. Cell death was assessed based on release of lactate dehydrogenase (LDH) using a cytotoxicity detection kit (Promega) using a protocol described previously (14,30,31). The experiments were repeated at least three times, and the representative results are shown in each figure.

Detection of ROS

Cells were treated with BPDE as shown in each figure legend. 5-(and-6)-Chloromethyl-2′,7′-dichlorodihydro fluorescein diacetate, acetyl ester (5 μM) was added to culture medium 30 min before cell harvest. ROS was measured with a fluorescence plate reader. The results were normalized with total protein concentration (31). All the experiments were repeated at least three times, and the representative results are shown in each figure.

Catalase activity detection

The cells were seeded in 12-well plate and cultured for 24 h before collection for preparing cell lysates in M2 buffer without dithiothreitol. Catalase activity was measured using the Amplex red catalase assay kit following the manufacturer's instruction. All the experiments were performed in triplicate.

Cell transformation assay

The procedure of cell transformation was as reported with modifications (32,33). HBEC-13 cells (1×10^4/well) were treated with BPDE (0.2 μM) every 2 days for 1 week (a total of 3 treatments). For each treatment, cells were exposed to BPDE for 1 h and then incubated in fresh medium. The cells were then seeded in soft agar for colony formation. Colonies in agar were photographed and counted after incubation for 2 weeks. The average number of colonies in six randomly selected fields was calculated. All experiments were run in triplicate.

Detection of RIP1 expression in mouse lung tumors and cigarette smoking-exposed mouse lung tissues

C57Bl/6 mice (14–24 weeks old) purchased from Charles River were exposed to cigarette smoking (CS) as we described previously using type 2R4F research cigarettes (Kentucky Tobacco Research and Development Center) for 4 weeks (6 h/day, 5 days/week) in Hazelton 1000 chambers. Exposure concentrations of total particulate material were 100 mg/m^3 for the first week and 250 mg/m^3 for subsequent 3 weeks. Age-matched control mice were housed in similar exposure chambers and exposed to filtered air (34). The mice were killed, and extracts from whole lung tissues were used for western blot. For inducing lung tumor, A/J mice (4–6 weeks old) were treated with a single dose of benzo(a)pyrene (100 mg/kg, intra peritoneally) and held for 42 weeks. Mouse lung tumor and matched lung tissues were used for western blot. All experiments were approved by the Institutional Animal Care and Use Committee and were performed at Lovelace Respiratory Research Institute, a facility approved by the Association for the Assessment and Accreditation for Laboratory Animal Care International.

Statistics

All data were expressed as means ± SD and examined by one-way analysis of variance for statistical significance. $P < 0.05$ was considered statistically significant.

Results

RIP1 expression is elevated in human lung tumors and was induced by BPDE or CSE in HBECs

To investigate the role of RIP1 in lung cancer development, we first examined RIP1 expression in human non-small cell lung cancer tumor tissues by immunohistochemistry. Although RIP1 was weakly detectable in normal lung tissues, increased RIP1 expression was detected in 34.8% of lung tumors: in 39.6% of adenocarcinoma and in 39.4% of squamous cell carcinoma (Figure 1A and B). Consistently, the expression level of RIP1 in mouse lung tumors was also increased compared with the matched lung tissues (Figure 1C). Increase of RIP1 expression in lung tumor tissues prompted us to investigate the potential role of RIP1 in human non-small cell lung cancer development.

Because most human lung cancers are associated with CS, we then examined if RIP1 expression in HBECs is impacted by cigarette smoke. Indeed, CS exposure remarkably increased RIP1 expression in mouse lung tissues (Figure 1D). Additionally, CSE potently induced RIP1 expression in HBEcs, which started as early as 4 h (Figure 1D, upper). Immunohistostaining was performed to examine RIP1 expression *in situ*. RIP1 was moderately expressed mainly in airway epithelial and alveolar cells in normal mouse lung, which was significantly increased after CS exposure (Supplementary Figure S1, available at *Carcinogenesis* Online). Interestingly, BPDE, an active metabolite of the cigarette smoke carcinogen benzo(a)pyrene, also strongly increased RIP1 expression in both HBEC-2 and HBEC-13 cells (Figure 1D, lower). The constitutive RIP1 expression was unchanged during the experimental time (Supplementary Figure S2, available at *Carcinogenesis* Online). Altogether, these results suggest that RIP1

A

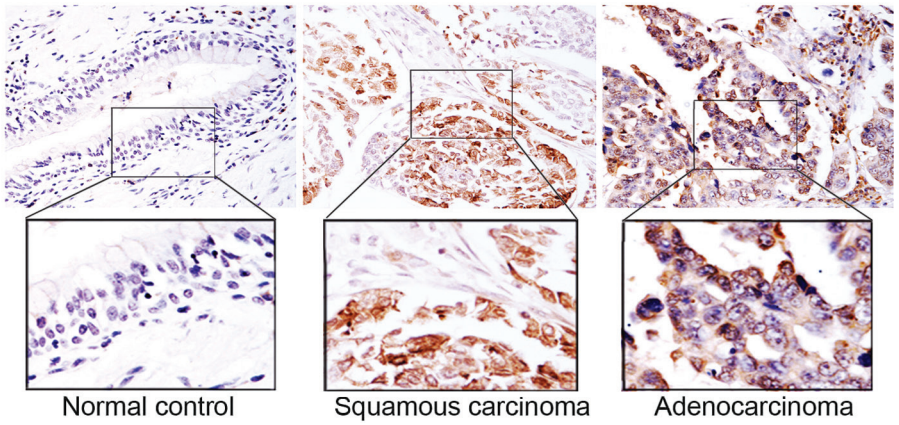

B

	Number	RIP1 increased(%)
Squamous cell carcinoma	99	39 (39.4%)
Adenocarcinoam	96	38 (39.6%)
Others	29	1 (3.45%)
Total	224	78 (34.8%)

C

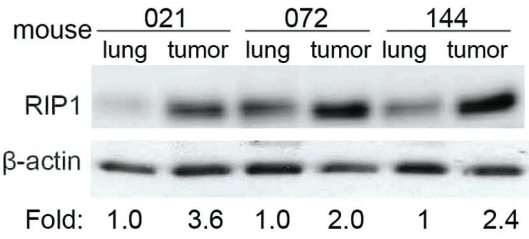

D

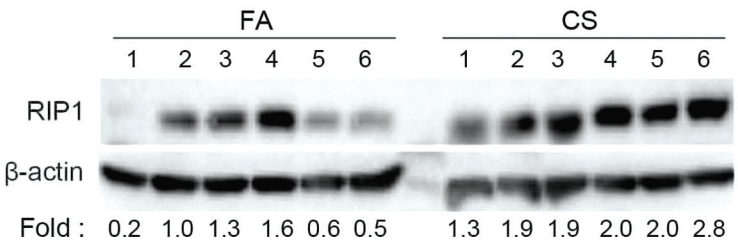

E

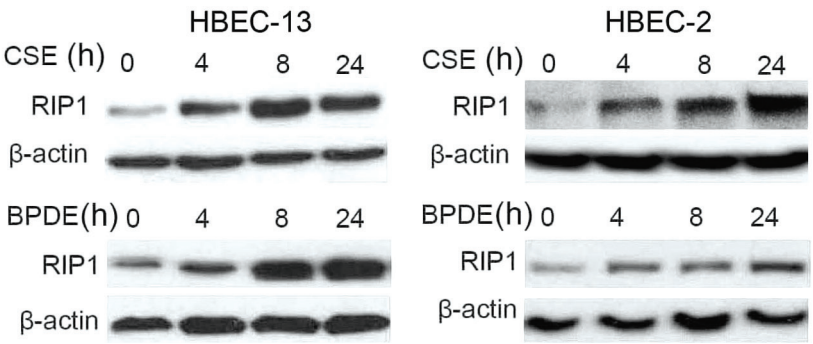

Fig. 1. Increased RIP1 expression in human lung cancer tissues, and cigarette carcinogen induces RIP1 expression in HBECs. (**A**), RIP1 expression was detected in a human non-small cell lung cancer tissue array by immunohistostaining. Representative images from normal lung, adenocarcinoma and squamous cell carcinoma are shown. (**B**) The summary of tumors with increased RIP1 expression. (**C**) RIP1 was detected in mouse tumors and matched lung tissues. The intensity of the individual bands was quantified by densitometry and normalized to the corresponding input control (β-actin) bands. Relative RIP1 expression was calculated with the respective lung tissues taken as 1. (**D**) RIP1 in lung tissues from six cigarette smoke and six control fresh air mice. Relative RIP1 expression levels shown were calculated as in (C). (**E**) HBEC-13 and HBEC-2 cells were treated with BPDE (0.2 μM) or CSE (10 μg/ml total particulate material) for indicated time points, RIP1 expression was detected by western blot. β-Actin was used as an input control.

may be involved in cigarette smoke-induced lung carcinogenesis. Because BPDE acts similarly as CSE in regulating RIP1 expression and is a potent carcinogen that induces HBEC transformation (32,33), we conducted the following experiments with BPDE.

Inhibiting RIP1 expression sensitizes HBECs to BPDE-induced cell cytotoxicity

Because RIP1 plays a crucial role in mediating cell survival and death signaling, we then examined if RIP1 ablation affects BPDE-induced cytotoxicity in HBECs. To this end, we stably transfected RIP1 shRNA into HBEC-2 and HBEC-13 to stably knockdown RIP1 expression (Figure 2A and B). The RIP1 shRNA had no effect on RIP3 expression, supporting the specificity of the shRNA (Supplementary Figure S3, available at *Carcinogenesis* Online). BPDE exposure resulted in cytotoxicity in both HBEC-2 and HBEC-13 cells in a dose-dependent manner (Figure 2A and B). Compared with the negative control shRNA-transfected cells that retain RIP1 expression, the RIP1 knockdown cell clones derived from both HBEC-2 and HBEC-13 cells showed significantly increased sensitivity to BPDE-induced cytotoxicity (Figure 2A and B). These results suggest that RIP1 plays a survival role in HBECs against BPDE-induced cell cytotoxicity.

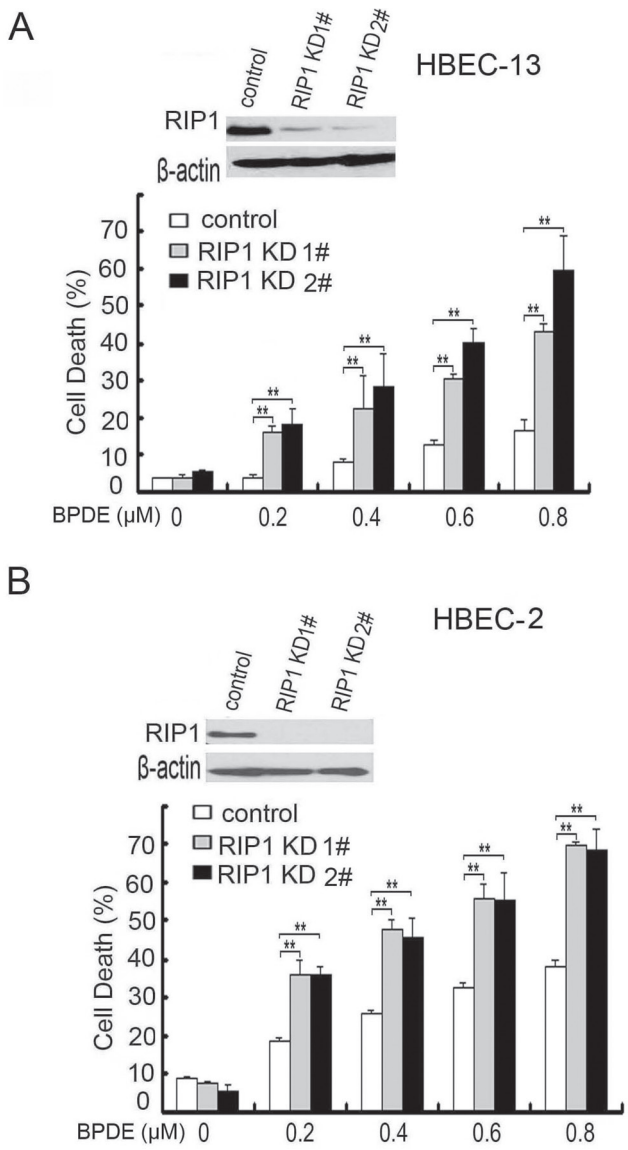

Fig. 2. RIP1 knockdown sensitizes HBECs to BPDE-induced cell cytotoxicity. (**A** and **B**) Cells were treated with increasing concentrations of BPDE for 36 h. Cell death was detected by LDH release assay. Data shown are mean ± SD. $^{**}P < 0.05$. Knockdown of RIP1 was confirmed by western blot. β-Actin was used as an input control.

RIP1 suppresses MAPK-mediated cytotoxicity induced by BPDE

RIP1 mediates cellular signaling for activation of MAPKs (JNK, ERK and p38), which are involved in cell survival and death control (3,17,19–21). Thus, we examined if MAPK activation induced by BPDE is regulated by RIP1. It was noticed that the basal level of ERK and JNK activity was increased in the RIP1 knockdown cells (Figure 3A and B; Supplementary Figure S4, available at *Carcinogenesis* Online). In both control HBEC-2 and HBEC-13 cells, BPDE slightly activated all the three MAPKs (Figure 3A and B). Strikingly, each two RIP1 knockdown cell clones derived from both HBEC-2 and HBEC-13 cells showed remarkably enhanced activation of JNK, ERK and p38 induced by BPDE (Figure 3A and B). The constitutive expression activity of these proteins was unchanged during the experimental time (Supplementary Figure S4, available at *Carcinogenesis* Online). To examine the role of MAPK in BPDE-induced cytotoxicity, we employed pharmacological inhibitors (SP600125 for JNK, SB203580 for p38 and U0126 for ERK) for blocking each MAPK. Although the inhibitors by themselves had little toxicity in either the control or RIP1 knockdown cells, they significantly reduced BPDE-induced cell death in RIP1-suppressed HBEC cell clones (Figure 3C and D). The efficiency of each inhibitor against its target MAPK was confirmed by western blot (Figure 3E) (35–38). Collectively, these results indicate that RIP1 suppresses MAPK-mediated cytotoxicity induced by BPDE in HBECs.

RIP1 suppresses BPDE-induced intracellular ROS accumulation in HBECs

BPDE is able to induce ROS, a messenger for cellular signaling to MAPK activation, and excessive ROS may result in cell death (39–41). Therefore, we examined if RIP1 is involved in regulating BPDE-induced ROS production. BPDE induced slight increase of ROS in control HBEC-2 and HBEC-13 cells. However, a significantly higher induction of ROS by BPDE in RIP1-suppressed cell clones was observed (Figure 4A and B), suggesting that RIP1 suppresses BPDE-induced oxidative stress in HBECs. Scavenging ROS with ROS scavengers NAC and BHA significantly attenuated BPDE-induced cell death in these RIP1-suppressed HBECs (Figure 4C and D). Interestingly, these ROS scavengers also remarkably suppressed BPDE-induced activation of all the MAPKs in RIP1 knockdown cells (Figure 4E). These results suggest that RIP1 suppresses BPDE-induced cytotoxicity through inhibiting ROS-mediated MAPK activation.

RIP1 maintains catalase expression that suppresses BPDE-induced ROS accumulation

ROS is mainly produced in mitochondria where electrons are leaked from the respiratory chain to form superoxide, which is converted to H_2O_2 by superoxide dismutases. Although the expression of manganese superoxide dismutase was moderately increased and marginal induction of superoxide was detected in BPDE-treated RIP1 knockdown HBECs (Figure 5A and data not shown), the expression of the H_2O_2 reducing enzyme catalase was dramatically decreased in RIP1 knockdown HBEC-2 and HBEC-13 cells (Figure 5A). Thus, we focused on catalase. Consistently, catalase activity in these cells was also significantly decreased (Figure 5B).

More importantly, application of catalase to the culture, which suppresses cellular ROS (42), efficiently blocked ROS accumulation and cytotoxicity induced by BPDE (Figure 5C and D). These results clearly show that RIP1 suppresses BPDE-induced ROS accumulation through maintaining catalase expression.

ERK- and JNK-mediated catalase degradation in RIP1 knockout HBECs

The expression of catalase is regulated by ubiquitination-mediated proteasomal degradation (43). Because K-ras^{G12V} that activates MAPKs

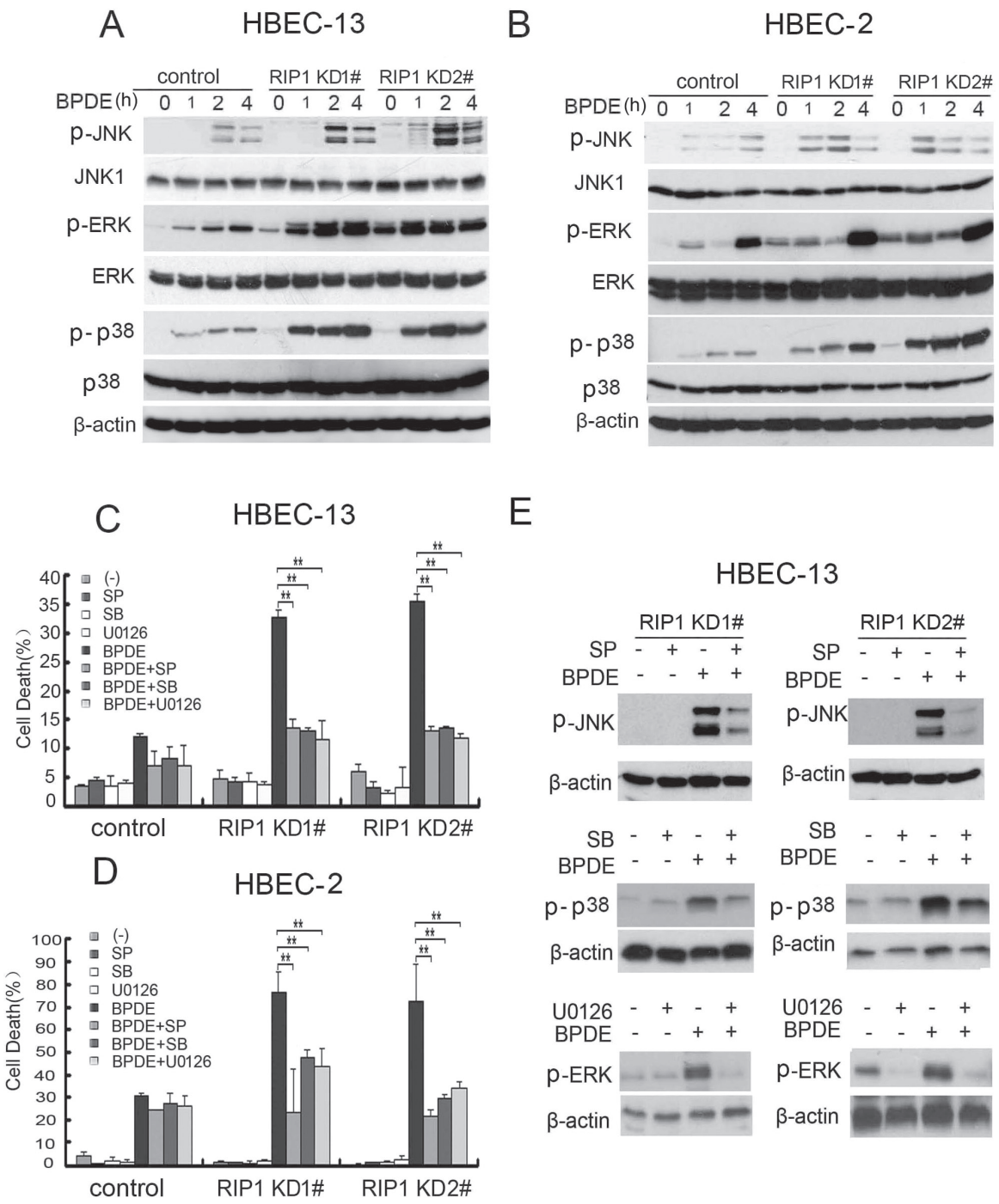

Fig. 3. RIP1 suppresses activation of MAPKs induced by BPDE. (**A** and **B**) RIP1 stable knockdown and control (negative shRNA transfected) cells were treated with BPDE (0.4 μM) for indicated times. The indicated proteins were detected by western blot. β-Actin was used as input control. (**C** and **D**) Cells were pretreated with indicated inhibitors (SP600125, 10 μM; SB203580, 10 μM; U0126, 10 μM) for 45 min and then treated with BPDE (0.4 μM) for another 36 h. Cell death was measured by LDH release assay. Data shown are mean ± SD. $^{**}P < 0.05$. (**E**) Cells were pretreated with indicated inhibitors (SP600125, 10 μM; SB203580, 10 μM; U0126, 10 μM) for 45 min, then treated with BPDE (0.4 μM) for an additional 4 h. The expression of indicated proteins was detected by western blot. β-Actin was used as the input control.

effectively suppressed catalase expression and our results showed increased MAPK activity in RIP1 knockdown HBECs (Figure 3A and B) (44), we next examined if these MAPKs are involved in catalase suppression when RIP1 is suppressed. Indeed, blocking ERK and JNK but not p38 effectively restored catalase expression in the RIP1 knockdown HBEC clones (Figure 6A). The stability of catalase in RIP1 knockdown cells is significantly reduced, which is shown as shortened half-life (1.2 h) compared with that of control cells (>8 h, Figure 6B). Further, the proteasome inhibitor MG132, but not the lysosome inhibitor chloroquine, strongly increased catalase expression in the RIP1 knockdown HBEC cells (Figure 6C), suggesting the decrease of catalase expression in RIP1 knockdown HBECs is through proteasomal degradation. Taken together, these results suggest that the increased ERK and JNK activity leads to proteasomal degradation of catalase in RIP1-suppressed HBECs.

Involvement of RIP1 in BPDE-induced cell transformation

Transformation of HBECs is a chronic process, which depends on survival of cells having acquired genetic and epigenetic alterations (32). Because RIP1 is important for HBEC survival during

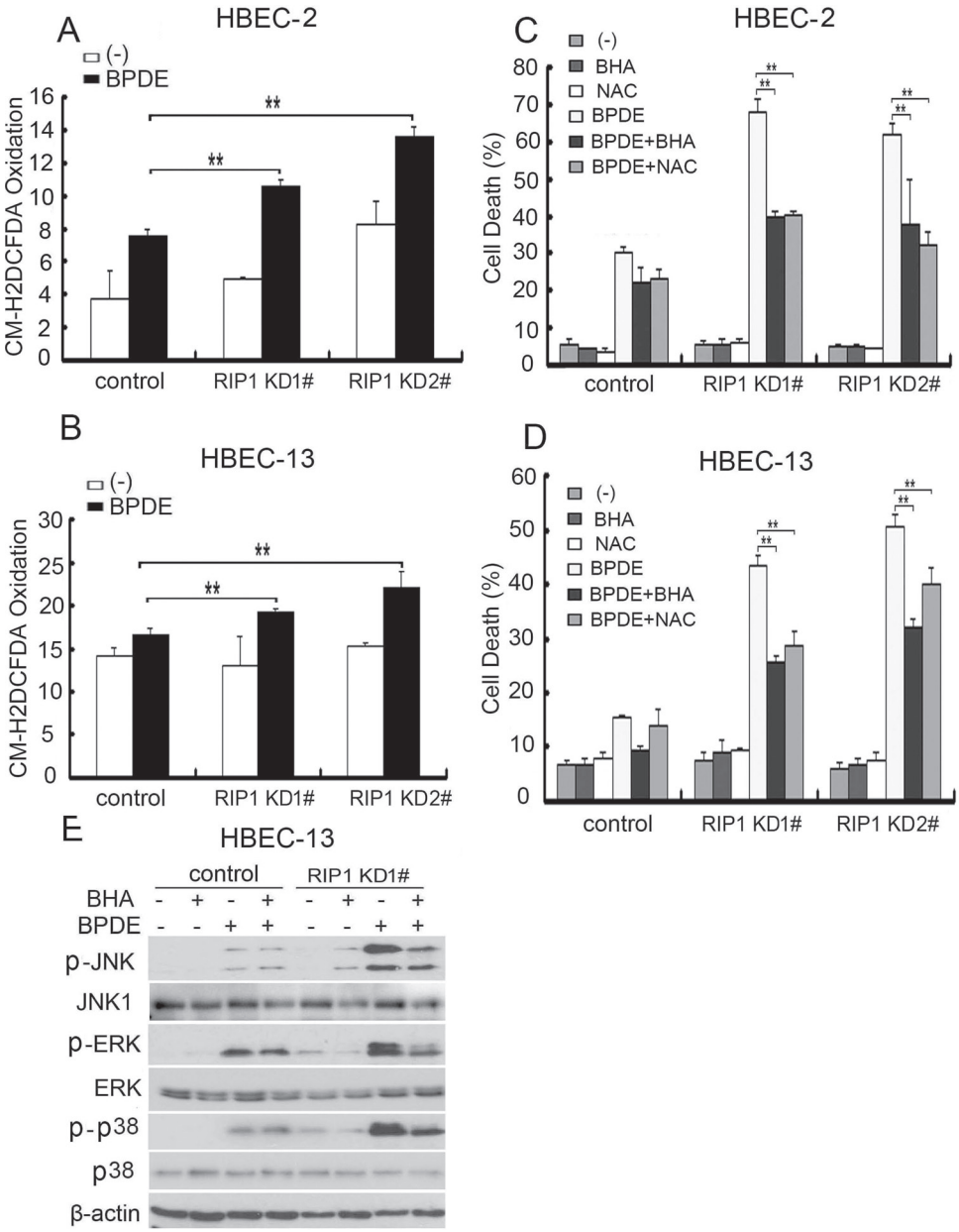

Fig. 4. BPDE-induced intracellular ROS accumulation contributes to potentiated MAPK activation in RIP1 knockdown cells. (**A** and **B**) Cells were treated with BPDE (0.4 μM) for 2 h and incubated with 5-(and-6)-chloromethyl-2′,7′-dichlorodihydro fluorescein diacetate, acetyl ester (5 μM) for 30 min before being collected for ROS detection. Data shown are the mean ± SD. $^{**}P < 0.05$. (**C** and **D**) Cells were pretreated with indicated ROS scavengers (BHA, 100 μM; NAC, 3 mM) for 45 min, then treated with BPDE (0.4 μM) for an additional 36 h. Cytotoxicity was detected by LDH release assay. Data shown are the mean ± SD. $^{**}P < 0.05$. (**E**) Cells were treated with BHA (100 μM) or NAC (3 mM) for 45 min followed by BPDE (0.4 μM) for another 4 h. The indicated proteins were detected by western blot. β-Actin was detected as the input control.

short-time BPDE exposure (Figure 2), we examined the effect of RIP1 knockdown on BPDE-induced cell transformation. HBEC-13 cells were used because this cell line is potently transformed as early as 1 week by BPDE. BPDE potently induced transformation of the negative control shRNA-transfected HBEC-13 cells, as shown by colony formation in soft agar (Figure 7A and B). The cell number seeded was 10 000 per well and the colony formation was about 400–600. The transformation efficiency was about 4–6%. Strikingly, RIP1 suppression in HBEC-13 cells strongly reduced BPDE-induced transformation (Figure 7A and B). Similar results were obtained in BEAS-2B cells, human bronchial epithelial cells immortalized with a distinct approach to that of HBEC-13 (Supplementary Figure S5, available at *Carcinogenesis* Online). Altogether, these results suggest that RIP1 plays an important role in promoting malignant transformation through protecting HBECs against carcinogen-induced cytotoxicity.

Discussion

In this report, for the first time, we show evidence attributing an oncogenic role to RIP1 in lung cancer: RIP1 expression was significantly increased in human lung cancer tissues and cell lines; RIP1 expression in HBEC was strongly stimulated by carcinogens CSE or BPDE; BPDE-induced cytotoxicity was significantly increased in RIP1 knockdown HBECs, which was associated with induction of ROS-mediated JNK activation; catalase expression was decreased in RIP1 knockdown HBECs; application of catalase to the culture effectively blocked BPDE-induced ROS accumulation and cytotoxicity; and

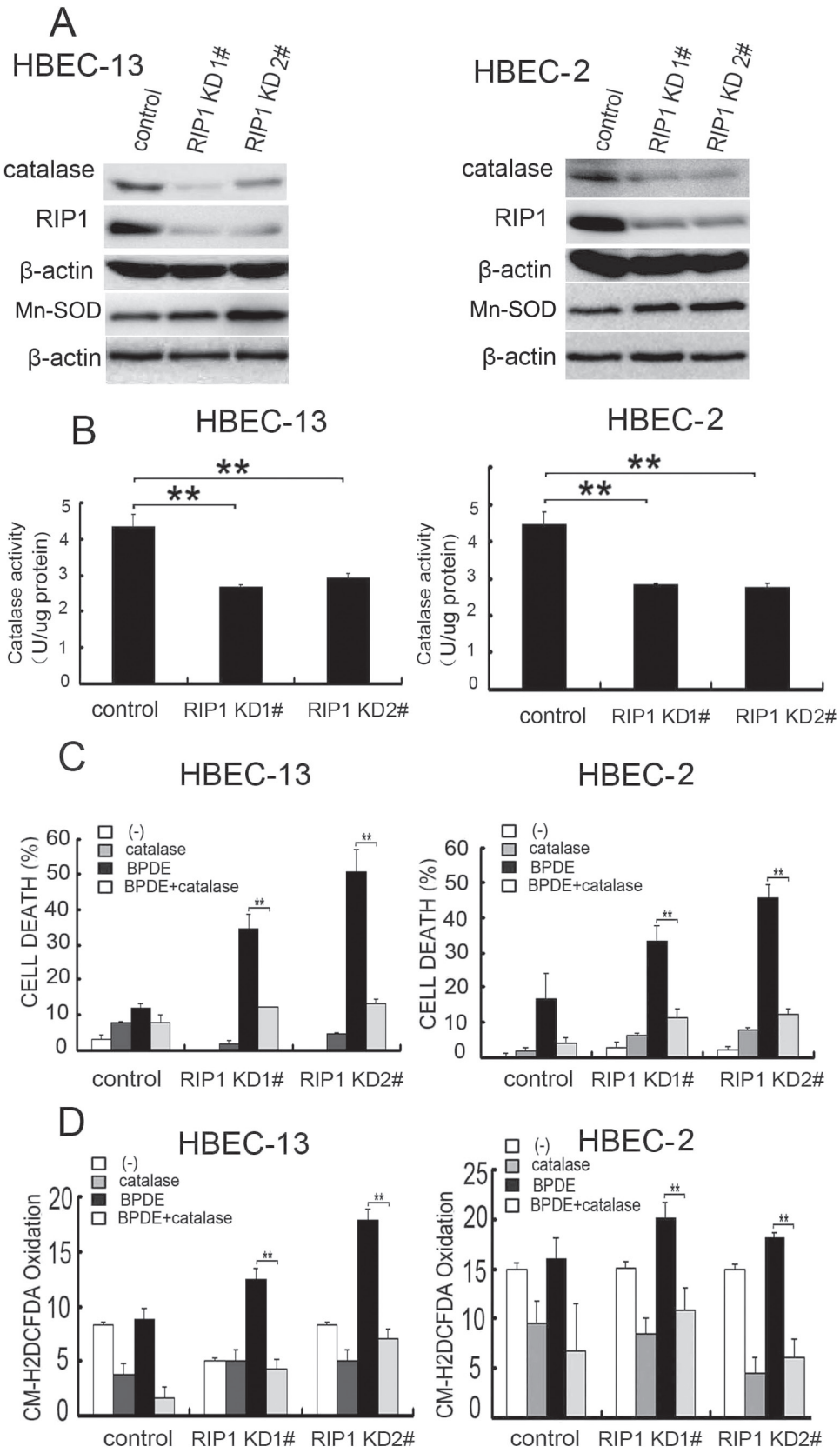

Fig. 5. Reduced catalase expression and activity in RIP1 knockdown cells are involved in BPDE-induced cytotoxicity. (**A**) Catalase and manganese superoxide dismutase expression was detected by western blot. β-Actin was detected as the input control. (**B**) Catalase activity was detected in the indicated cells. Data shown are the average of triplicates and mean ± SD. $^{**}P < 0.05$. (**C**) Cells were treated with exogenous catalase (250 U/ml) and BPDE (0.4 μM) or remained untreated for 36 h. Cell cytotoxicity was detected by LDH release assay. Data shown are the mean ± SD. $^{**}P < 0.05$. (**D**) The cells were treated with catalase (250 U/ml) and BPDE (0.4 μM) for 2 h. ROS was detected with fluorescence plate reader. Data shown are the mean ± SD. $^{**}P < 0.05$.

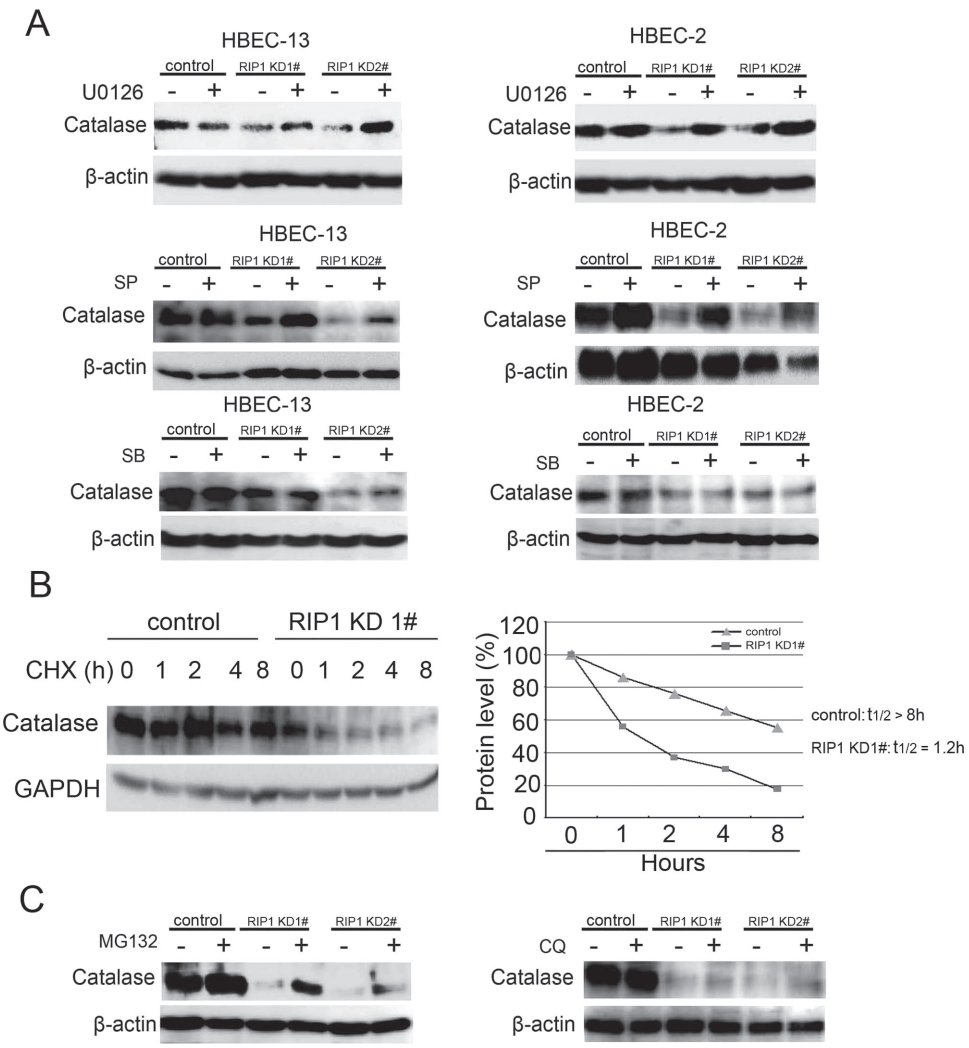

Fig. 6. JNK and ERK mediate catalase degradation in RIP1 knockdown cells. (**A**) Cells were treated with indicated inhibitors (U0126, 10 μM; SP600125, 10 μM; CSB203580, 10 μM) for 16 h. The expression of catalase was detected by western blot. β-Actin was detected as the input control. (**B**) Left, cells were treated with cycloheximide (10 μg/ml) for the indicated times. Catalase and β-actin were detected by western blot. Right, quantification of the results in Left. The intensity of the individual bands was quantified by densitometry (NIH Image 1.62) and normalized to the corresponding input control (β-actin) bands. (**C**) HBEC-2 cells were treated with the proteasome inhibitor MG132 (10 μM) or lysosome inhibitor chloroquine (20 μM) for 16 h. Catalase was detected by western blot. β-Actin was detected as the input control.

BPDE-induced transformation of HBECs was significantly reduced in RIP1 knockdown HBECs. Our results strongly suggest that RIP1 promotes malignant transformation through protecting DNA-damaged cells against carcinogen-induced cytotoxicity associated with excessive ROS production (Figure 7C).

As an important signaling integrator for different pathways that are involved in carcinogenesis, the role of RIP1 in carcinogenesis has not been well elucidated. Because the pro- and antisurvival signaling converge at RIP1, either a pro- or anticancer role may be plausible. In this study, we strongly suggest a procancer role for RIP1 in human lung epithelial cells, which involves cell survival and transformation during the course of carcinogen exposure. Our finding is consistent with previous reports suggesting a tumor-promoting role of RIP1 in glioblastoma, which may involve activation of NF-κB and Akt or inhibition of p53 (25,26). In our study, we found that suppression of excessive ROS production and MAPK-mediated apoptotic cell death underlies the mechanism of RIP1's effect on BPDE-induced HBEC transformation. BPDE slightly activated the NF-κB pathway, which was abolished when RIP1 was suppressed (Supplementary Figure S6, available at *Carcinogenesis* Online). Although whether NF-κB is involved in ROS-mediated MAPK activation needs further study, our model places RIP1 at the pivotal point for carcinogen-induced oncogenic transformation. The mediation of cell survival signaling by RIP1 appears to be important for maintaining the viability of DNA-damaged cells during carcinogen challenge, which results in outgrowth of cells with acquired gene mutation and epigenetic alterations for lung cancer development (Figure 7C).

We found that there is increased ROS production in RIP1 knockdown HBECs, suggesting a role for RIP1 in maintaining redox homeostasis. Although a clear ROS-suppressing role for RIP1 is seen in this study, RIP1 was found to mediate TNFα-induced ROS accumulation in mouse embryonic fibroblasts (17). This discrepancy suggests that role of RIP1 role in ROS regulation is complex, which may be dependent on cell or stimulation types. It is worth noting that the RIP1-mediated ROS induced by TNFα is mainly superoxide, which may be produced through mitochondrial respiration or cell membrane nicotinamide adenine dinucleotide phosphate oxidase (45). The increase of BPDE-induced ROS in RIP1 knockdown HBECs appears to involve catalase. While how RIP1 maintains the expression level of catalase has not been fully understood, our results clearly show that the increased ERK and JNK activity promotes catalase degradation at the proteasome in RIP1-suppressed HBEC cells. Thus, RIP1 loss establishes a positive feedback loop for ROS-mediated cell death involving ERK- and JNK-mediated catalase degradation. Our work

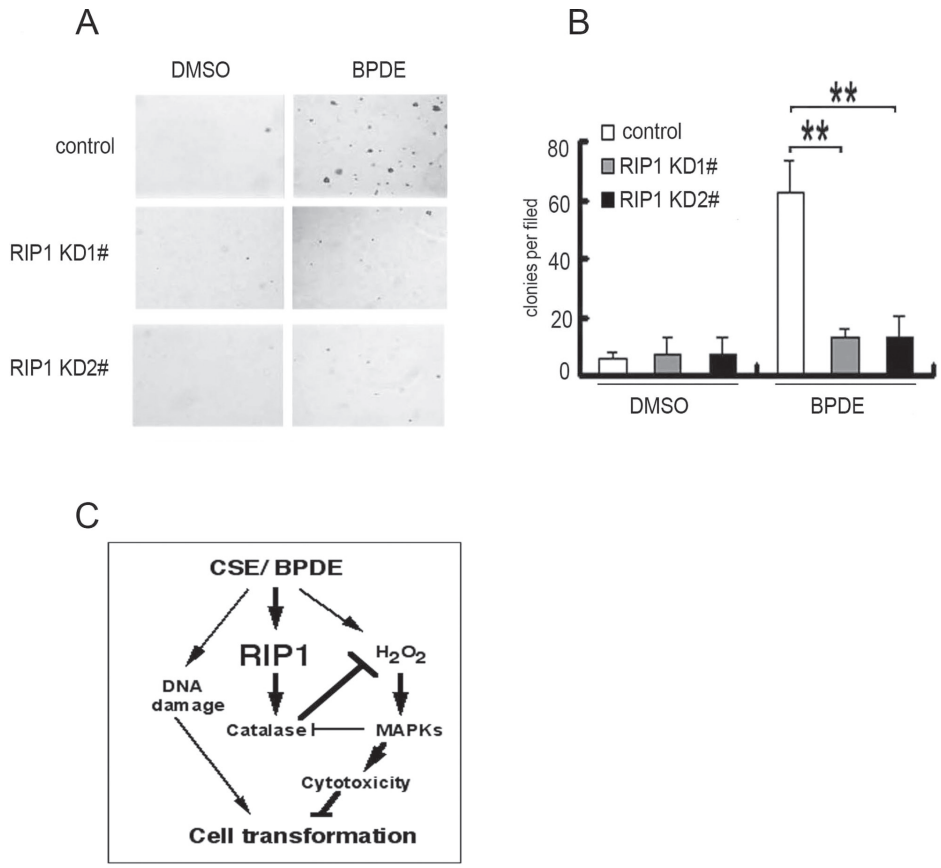

Fig. 7. RIP1 knockdown suppresses BPDE-induced transformation in HBEC-13 cells. (**A**) Cells (1×10^4) were seeded in 6-well plates and treated with BPDE (0.2 μM) every 2 days for 1 week or remained untreated, then seeded in soft agar and incubated for 2 weeks. Representative images are shown. (**B**) Quantitative representation of colony formation in soft agar. Bars show the averages of colony numbers of six randomly selected fields. Data shown are mean ± SD. $^{**}P < 0.01$. (**C**) A model of RIP1 in BPDE-induced lung carcinogenesis. RIP1 expression is increased by cigarette smoke carcinogens, which stabilizes catalase, resulting in suppression of ROS accumulation and MAPK activation-mediated cytotoxicity in DNA-damaged bronchial epithelial cells. This process facilitates cell survival and contributes to malignant transformation.

identifies a RIP1/catalase cascade that plays a procancer role in ensuring cell survival and transformation (Figure 7C).

ROS is usually generated in mitochondria and serves as a second messenger for cellular signaling (40). ROS also damages DNA, lipids and protein, contributing to the pathogenesis of cancer. However, excessive production of ROS that leads to extensive damage of cellular components will result in cell death, either apoptosis or necrosis (46–48). ROS can serve as a direct activator of cell death or as a second messenger that mediates cell death signals induced by stimuli such as anticancer chemotherapeutic agents and ionizing radiation. ROS are utilized for anticancer therapy (49). In a similar scenario, we propose that excessive ROS induction in DNA-damaged cells would eliminate these cancer-prone cells to prevent cancer. Therefore, suppressing the excessive ROS production caused by cigarette smoke would be oncogenic. Indeed, the transformation results with RIP1 knockdown HBECs in this study fully substantiate this hypothesis.

In summary, our results for the first time suggest that RIP1 plays an oncogenic role in the lung through maintaining survival of lung epithelial cells that have acquired genetic mutations and epigenetic alterations caused by carcinogens. Further studies with animal models are warranted for validating this novel oncogenic function for RIP1.

Supplementary material

Supplementary Figures S1–S6 can be found at http://carcin.oxfordjournals.org/

Funding

National Institute of Environmental Health Sciences/National Institutes of Health (R01ES017328); National Natural Science Foundation of China (30973403).

Conflict of Interest Statement: None declared.

References

1. Hanahan,D. *et al.* (2011) Hallmarks of cancer: the next generation. *Cell*, **144**, 646–674.
2. Festjens,N. *et al.* (2007) RIP1, a kinase on the crossroads of a cell's decision to live or die. *Cell Death Differ.*, **14**, 400–410.
3. Meylan,E. *et al.* (2004) RIP1 is an essential mediator of Toll-like receptor 3-induced NF-kappa B activation. *Nat. Immunol.*, **5**, 503–507.
4. Zhang,J. *et al.* (2011) RIP1-mediated regulation of lymphocyte survival and death responses. *Immunol. Res.*, **51**, 227–236.
5. Kelliher,M.A. *et al.* (1998) The death domain kinase RIP mediates the TNF-induced NF-kappaB signal. *Immunity*, **8**, 297–303.
6. Ting,A.T. *et al.* (1996) RIP mediates tumor necrosis factor receptor 1 activation of NF-kappaB but not Fas/APO-1-initiated apoptosis. *EMBO J.*, **15**, 6189–6196.
7. Lin,Y. *et al.* (2000) The death domain kinase RIP is essential for TRAIL (Apo2L)-induced activation of IkappaB kinase and c-Jun N-terminal kinase. *Mol. Cell. Biol.*, **20**, 6638–6645.
8. Kaiser,W.J. *et al.* (2005) Apoptosis induced by the toll-like receptor adaptor TRIF is dependent on its receptor interacting protein homotypic interaction motif. *J. Immunol.*, **174**, 4942–4952.
9. Meylan,E. *et al.* (2005) The RIP kinases: crucial integrators of cellular stress. *Trends Biochem. Sci.*, **30**, 151–159.

10. Hur,G.M. *et al.* (2003) The death domain kinase RIP has an essential role in DNA damage-induced NF-kappa B activation. *Genes Dev*., **17**, 873–882.
11. Park,J. *et al.* (2012) ARD1 binding to RIP1 mediates doxorubicin-induced NF-κB activation. *Biochem. Biophys. Res. Commun*., **422**, 291–297.
12. Bai,L. *et al.* (2011) Blocking NF-κB and Akt by Hsp90 inhibition sensitizes Smac mimetic compound 3-induced extrinsic apoptosis pathway and results in synergistic cancer cell death. *Apoptosis*, **16**, 45–54.
13. Palacios,C. *et al.* (2010) Down-regulation of RIP expression by 17-dimethylaminoethylamino-17-demethoxygeldanamycin promotes TRAIL-induced apoptosis in breast tumor cells. *Cancer Lett*., **287**, 207–215.
14. Wang,X. *et al.* (2006) 17-Allylamino-17-demethoxygeldanamycin synergistically potentiates tumor necrosis factor-induced lung cancer cell death by blocking the nuclear factor-kappaB pathway. *Cancer Res*., **66**, 1089–1095.
15. Wang,L. *et al.* (2008) TNF-alpha induces two distinct caspase-8 activation pathways. *Cell*, **133**, 693–703.
16. Holler,N. *et al.* (2000) Fas triggers an alternative, caspase-8-independent cell death pathway using the kinase RIP as effector molecule. *Nat. Immunol*., **1**, 489–495.
17. Lin,Y. *et al.* (2004) Tumor necrosis factor-induced nonapoptotic cell death requires receptor-interacting protein-mediated cellular reactive oxygen species accumulation. *J. Biol. Chem*., **279**, 10822–10828.
18. Tenev,T. *et al.* (2011) The Ripoptosome, a signaling platform that assembles in response to genotoxic stress and loss of IAPs. *Mol. Cell*, **43**, 432–448.
19. Devin,A. *et al.* (2003) The role of the death-domain kinase RIP in tumour-necrosis-factor-induced activation of mitogen-activated protein kinases. *EMBO Rep*., **4**, 623–627.
20. Ventura,J.J. *et al.* (2004) JNK potentiates TNF-stimulated necrosis by increasing the production of cytotoxic reactive oxygen species. *Genes Dev*., **18**, 2905–2915.
21. Lee,T.H. *et al.* (2003) The death domain kinase RIP1 is essential for tumor necrosis factor alpha signaling to p38 mitogen-activated protein kinase. *Mol. Cell. Biol*., **23**, 8377–8385.
22. Lin,Y. *et al.* (1999) Cleavage of the death domain kinase RIP by caspase-8 prompts TNF-induced apoptosis. *Genes Dev*., **13**, 2514–2526.
23. Darding,M. *et al.* (2012) IAPs: guardians of RIPK1. *Cell Death Differ*., **19**, 58–66.
24. O'Donnell,M.A. *et al.* (2011) RIP1 comes back to life as a cell death regulator in TNFR1 signaling. *FEBS J*., **278**, 877–887.
25. Park,S. *et al.* (2009) The receptor interacting protein 1 inhibits p53 induction through NF-kappaB activation and confers a worse prognosis in glioblastoma. *Cancer Res*., **69**, 2809–2816.
26. Park,S. *et al.* (2009) RIP1 activates PI3K-Akt via a dual mechanism involving NF-kappaB-mediated inhibition of the mTOR-S6K-IRS1 negative feedback loop and down-regulation of PTEN. *Cancer Res*., **69**, 4107–4111.
27. Guza,R. *et al.* (2011) Influence of C-5 substituted cytosine and related nucleoside analogs on the formation of benzo[a]pyrene diol epoxide-dG adducts at CG base pairs of DNA. *Nucleic Acids Res*., **39**, 3988–4006.
28. Ding,J. *et al.* (2006) Effects of polycyclic aromatic hydrocarbons (PAHs) on vascular endothelial growth factor induction through phosphatidylinositol 3-kinase/AP-1-dependent, HIF-1alpha-independent pathway. *J. Biol. Chem*., **281**, 9093–9100.
29. Ramirez,R.D. *et al.* (2004) Immortalization of human bronchial epithelial cells in the absence of viral oncoproteins. *Cancer Res*., **64**, 9027–9034.
30. Wang,X. *et al.* (2007) Sensitization of TNF-induced cytotoxicity in lung cancer cells by concurrent suppression of the NF-kappaB and Akt pathways. *Biochem. Biophys. Res. Commun*., **355**, 807–812.
31. Ju,W. *et al.* (2007) A critical role of luteolin-induced reactive oxygen species in blockage of tumor necrosis factor-activated nuclear factor-kappaB pathway and sensitization of apoptosis in lung cancer cells. *Mol. Pharmacol*., **71**, 1381–1388.
32. Damiani,L.A. *et al.* (2008) Carcinogen-induced gene promoter hypermethylation is mediated by DNMT1 and causal for transformation of immortalized bronchial epithelial cells. *Cancer Res*., **68**, 9005–9014.
33. Xu,X. *et al.* (2012) MUC1 contributes to BPDE-induced human bronchial epithelial cell transformation through facilitating EGFR activation. *PLoS One*, **7**, e33846.
34. Nyunoya,T. *et al.* (2011) Antioxidant diet protects against emphysema, but increases mortality in cigarette smoke-exposed mice. *COPD*, **8**, 362–368.
35. Jablonska,E. *et al.* (2010) Transforming growth factor-β1 induces expression of human coagulation factor XII via Smad3 and JNK signaling pathways in human lung fibroblasts. *J. Biol. Chem*., **285**, 11638–11651.
36. Karahashi,H. *et al.* (2009) Lipopolysaccharide-induced apoptosis in transformed bovine brain endothelial cells and human dermal microvessel endothelial cells: the role of JNK. *J. Immunol*., **182**, 7280–7286.
37. Makeeva,N. *et al.* (2007) Role of TAB1 in nitric oxide-induced p38 activation in insulin-producing cells. *Int. J. Biol. Sci*., **3**, 71–76.
38. Li,Z. *et al.* (2011) Epidermal growth factor receptor-mediated tissue transglutaminase overexpression couples acquired tumor necrosis factor-related apoptosis-inducing ligand resistance and migration through c-FLIP and MMP-9 proteins in lung cancer cells. *J. Biol. Chem*., **286**, 21164–21172.
39. Gao,D. *et al.* (2005) Benzo[a]pyrene and its metabolites combined with ultraviolet A synergistically induce 8-hydroxy-2'-deoxyguanosine via reactive oxygen species. *Free Radic. Biol. Med*., **39**, 1177–1183.
40. Nimnual,A.S. *et al.* (2003) Redox-dependent downregulation of Rho by Rac. *Nat. Cell Biol*., **5**, 236–241.
41. Lin,A. *et al.* (2002) The true face of JNK activation in apoptosis. *Aging Cell*, **1**, 112–116.
42. Morel,Y. *et al.* (1999) An autoregulatory loop controlling CYP1A1 gene expression: role of H(2)O(2) and NFI. *Mol. Cell. Biol*., **19**, 6825–6832.
43. Cao,C. *et al.* (2003) Catalase is regulated by ubiquitination and proteosomal degradation. Role of the c-Abl and Arg tyrosine kinases. *Biochemistry*, **42**, 10348–10353.
44. Hu,Y. *et al.* (2012) K-ras(G12V) transformation leads to mitochondrial dysfunction and a metabolic switch from oxidative phosphorylation to glycolysis. *Cell Res*., **22**, 399–412.
45. Kim,Y.S. *et al.* (2007) TNF-induced activation of the Nox1 NADPH oxidase and its role in the induction of necrotic cell death. *Mol. Cell*, **26**, 675–687.
46. Shen,H.M. *et al.* (2004) Essential roles of receptor-interacting protein and TRAF2 in oxidative stress-induced cell death. *Mol. Cell. Biol*., **24**, 5914–5922.
47. Gardner,A.M. *et al.* (1997) Apoptotic vs. nonapoptotic cytotoxicity induced by hydrogen peroxide. *Free Radic. Biol. Med*., **22**, 73–83.
48. Bai,L. *et al.* (2012) A superoxide-mediated mitogen-activated protein kinase phosphatase-1 degradation and c-Jun NH(2)-terminal kinase activation pathway for luteolin-induced lung cancer cytotoxicity. *Mol. Pharmacol*., **81**, 549–555.
49. Trachootham,D. *et al.* (2009) Targeting cancer cells by ROS-mediated mechanisms: a radical therapeutic approach? *Nat. Rev. Drug Discov*., **8**, 579–591.

Received December 17, 2012; revised April 18, 2013; accepted April 25, 2013